molecules

MDPI

Article

Investigations of Antioxidant and Anti-Cancer Activities of 5-Aminopyrazole Derivatives

Federica Rapetti [1], Andrea Spallarossa [1], Eleonora Russo [1], Debora Caviglia [1], Carla Villa [1], Bruno Tasso [1], Maria Grazia Signorello [2], Camillo Rosano [3], Erika Iervasi [3], Marco Ponassi [3] and Chiara Brullo [1,*]

[1] Department of Pharmacy (DIFAR), University of Genoa, Viale Benedetto XV, 3, 16132 Genoa, Italy; federica.rapetti@unige.it (F.R.); andrea.spallarossa@unige.it (A.S.); eleonora.russo@unige.it (E.R.); debora.caviglia@edu.unige.it (D.C.); carla.villa@unige.it (C.V.); bruno.tasso@unige.it (B.T.)
[2] Department of Pharmacy (DIFAR), Biochemistry Lab., University of Genoa, Viale Benedetto XV, 3, 16132 Genova, Italy; mariagrazia.signorello@unige.it
[3] IRCCS Ospedale Policlinico San Martino, Proteomics and Mass Spectrometry Unit, L.go. R. Benzi, 10, 16132 Genova, Italy; camillo.rosano@hsanmartino.it (C.R.); iervasierika@gmail.com (E.I.); marco.ponassi@hsanmartino.it (M.P.)
* Correspondence: chiara.brullo@unige.it

Abstract: To further extend the structure-activity relationships (SARs) of 5-aminopyrazoles (5APs) and identify novel compounds able to interfere with inflammation, oxidative stress, and tumorigenesis, 5APs **1–4** have been designed and prepared. Some chemical modifications have been inserted on cathecol function or in aminopyrazole central core; in detail: (i) smaller, bigger, and more lipophilic substituents were introduced in *meta* and *para* positions of catechol portion (5APs **1**); (ii) a methyl group was inserted on C3 of the pyrazole scaffold (5APs **2**); (iii) a more flexible alkyl chain was inserted on N1 position (5APs **3**); (iv) the acylhydrazonic linker was moved from position 4 to position 3 of the pyrazole scaffold (5APs **4**). All new derivatives **1–4** have been tested for radical scavenging (DPPH assay), anti-aggregating/antioxidant (in human platelets) and cell growth inhibitory activity (MTT assay) properties. In addition, in silico pharmacokinetics, drug-likeness properties, and toxicity have been calculated. 5APs **1** emerged to be promising anti-proliferative agents, able to suppress the growth of specific cancer cell lines. Furthermore, derivatives **3** remarkably inhibited ROS production in platelets and 5APs **4** showed interesting in vitro radical scavenging properties. Overall, the collected results further confirm the pharmaceutical potentials of this class of compounds and support future studies for the development of novel anti-proliferative and antioxidant agents.

Keywords: 5-aminopyrazoles; MTT test; anti-cancer activity; DPPH; ROS; druglike properties

Citation: Rapetti, F.; Spallarossa, A.; Russo, E.; Caviglia, D.; Villa, C.; Tasso, B.; Signorello, M.G.; Rosano, C.; Iervasi, E.; Ponassi, M.; et al. Investigations of Antioxidant and Anti-Cancer Activities of 5-Aminopyrazole Derivatives. *Molecules* **2024**, *29*, 2298. https://doi.org/10.3390/molecules29102298

Academic Editor: Maria Emília De Sousa

Received: 4 April 2024
Revised: 9 May 2024
Accepted: 11 May 2024
Published: 14 May 2024

1. Introduction

Pyrazole nucleus has been extensively investigated as pharmacophore [1–11] and several aminopyrazoles bearing a free amino group showed relevant biological activity in different therapeutic areas [12–16]. Specifically, 5-aminopyrazoles (5APs) have been deeply studied for their anti-inflammatory and anticancer activity [17,18], providing useful ligands for receptors or enzymes, as p38 MAPK [19–22], COX [23], carbonic anhydrase [24], and other different targets involved in cancer progression [25,26], as demonstrated by the recent approval of 5AP **Pirtobrutinib**, a reversible BTK inhibitor, clinically used for the treatment of mantle cell lymphoma (MCL) [27–33].

In the effort to synthetize new pyrazole-based compounds able to interfere with inflammation, oxidative stress, and tumorigenesis, we recently reported derivatives **I** (Figure 1) endowed with excellent anti-proliferative activity. Molecular docking and molecular dynamic simulations suggested the ability of the most active compound **Ia** (Figure 1) to interact with polymeric tubulin α/tubulin β/stathmin4 complex at the colchicine binding site [34]. By applying a ring opening strategy, we obtained 5APs **II** (Figure 1), able to

strongly inhibit ROS and superoxide anion production, lipid peroxidation, and NADPH oxidase in thrombin-stimulated human platelets and ROS formation in EAhy926 cells [35].

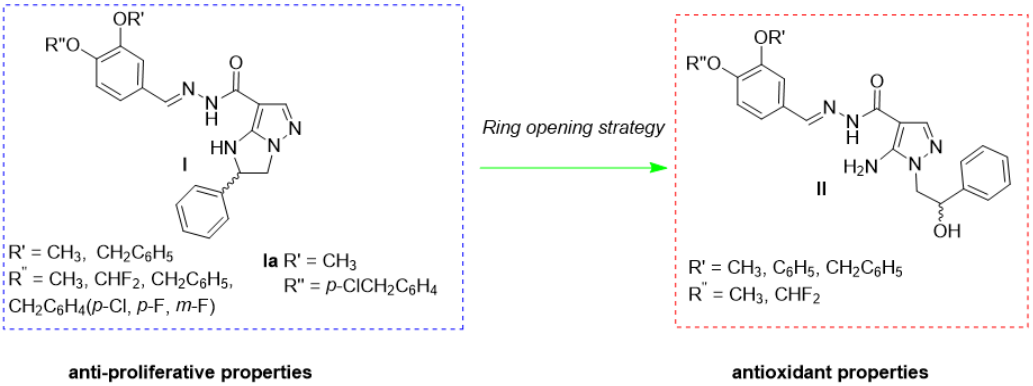

Figure 1. Chemical structure of previous compounds **I** and derived 5APs **II**.

To further extend the structure-activity relationships (SARs) of this class of compounds and verify their biological profile, a new library (eighteen compounds) of 5APs **1–4** was designed and synthesized (Figure 2 and Table 1). In detail: (i) in 5APs **1,** smaller, bigger, and more lipophilic substituents, similar to previous **II**, were introduced in *meta* and *para* positions of catechol portion; (ii) in 5APs **2**, a methyl group on C3 of the pyrazole scaffold was inserted to increase steric hindrance; (iii) in 5APs **3**, a more flexible alkyl chain was inserted on N1 position; (iv) finally, in 5APs **4**, the acylhydrazonic substituent was shifted from position 4 to position 3 of the pyrazole scaffold.

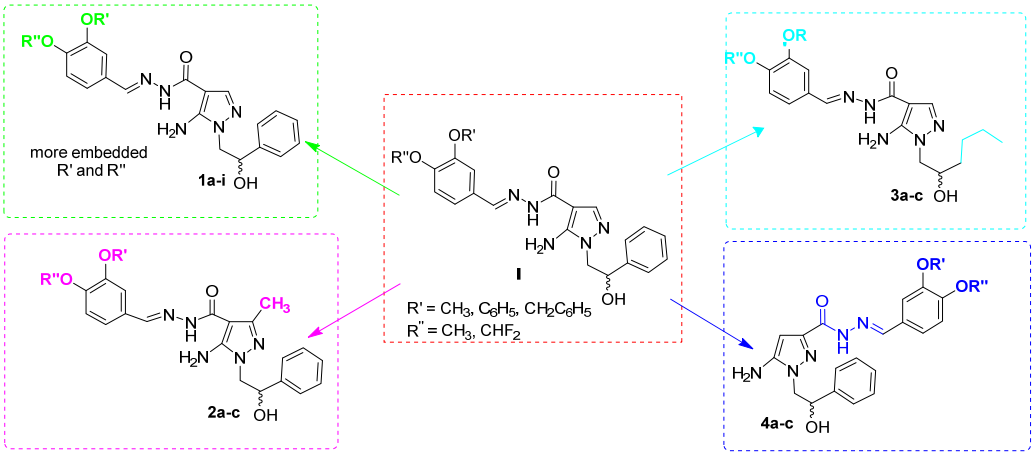

Figure 2. Chemical structure of previous 5-APs **I** and new 5APs **1–4**.

Table 1. Different decoration of novel compounds **1–4**.

Compounds	R′	R″
1a	//	CH_3
1b	CH_3	CH_3
1c	C_6H_5	CH_3
1d	$CH_2C_6H_5$	CH_3
1e	CH_3	$CH_2C_6H_4$-*p*F
1f	CH_3	$CH_2C_6H_4$-*m*F
1g	CH_3	$CH_2C_6H_4$-*p*Cl
1h	$CH_2C_6H_4$-*m*F	CHF_2
1i	$CH_2C_6H_4$-*p*Cl	CHF_2
2a	CH_3	CHF_2

Table 1. *Cont.*

Compounds	R′	R″
2b	C_6H_5	CHF_2
2c	$CH_2C_6H_5$	CHF_2
3a	CH_3	CHF_2
3b	C_6H_5	CHF_2
3c	$CH_2C_6H_5$	CHF_2
4a	CH_3	CHF_2
4b	C_6H_5	CHF_2
4c	$CH_2C_6H_5$	CHF_2

With the aim to investigate the antioxidant and anti-cancer activity of this novel library, in analogy with previous derivatives **I** and **II**, all new derivatives **1–4** have been tested for: (i) in vitro radical-scavenging activity (DPPH test); (ii) anti-aggregating/antioxidant activity in human platelets; and (iii) cell growth inhibitory activity. In addition, in silico pharmacokinetics, drug-likeness properties, and toxicity have been calculated.

2. Results

2.1. Chemistry

5APs **1–4** were synthesized in good-to-moderate yields through the three-step sequential procedure (Scheme 1). Briefly, the condensation of the proper ethyl cyanoacrylate **5a–c** with suitable hydrazinoethanol **6a,b** [36–38] led to 5APs **7a–d**, as previously reported [37–39]. These intermediates were then transformed in the corresponding hydrazides **8a–d** by reaction with hydrazine monohydrate. Finally, the reaction between carbohydrazide intermediates **8** and the suitable benzaldehydes **9a–l** (commercially available or prepared via literature methods [40,41]) allowed the isolation of the desired compounds **1–4** (Table 1).

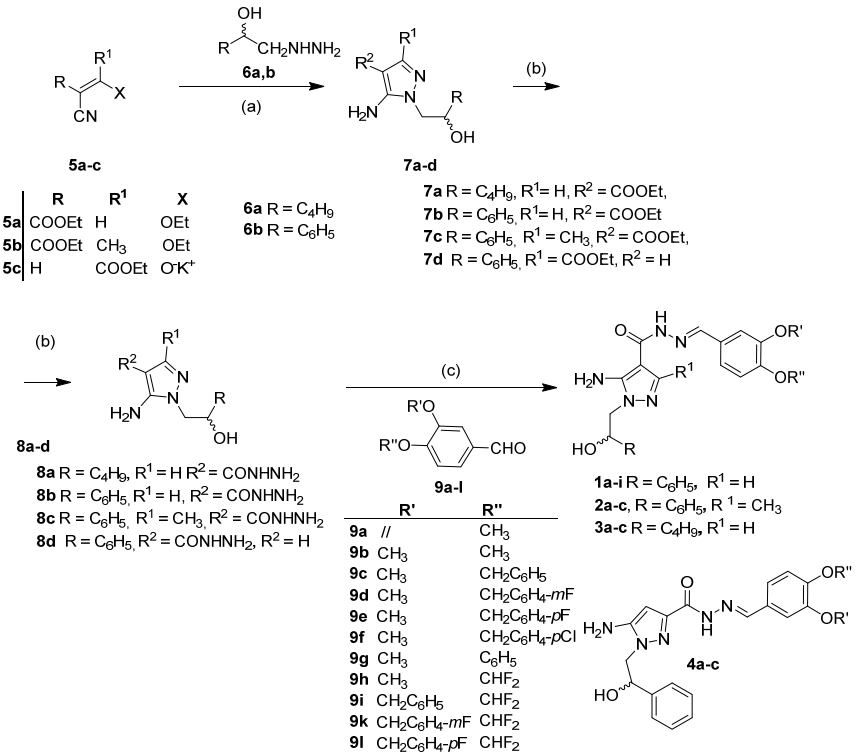

	R	R1	X
5a	COOEt	H	OEt
5b	COOEt	CH_3	OEt
5c	H	COOEt	O^-K^+

	R'	R''
9a	//	CH_3
9b	CH_3	CH_3
9c	CH_3	$CH_2C_6H_5$
9d	CH_3	$CH_2C_6H_4$-*m*F
9e	CH_3	$CH_2C_6H_4$-*p*F
9f	CH_3	$CH_2C_6H_4$-*p*Cl
9g	CH_3	C_6H_5
9h	CH_3	CHF_2
9i	$CH_2C_6H_5$	CHF_2
9k	$CH_2C_6H_4$-*m*F	CHF_2
9l	$CH_2C_6H_4$-*p*F	CHF_2

Scheme 1. Synthesis of compounds **1–4**. Reagents and conditions: (a) Toluene, 70–80 °C, 8 h (**7b**, **7d**) or absolute ethanol (abs. EtOH), reflux (**7a**, **7c**); (b) $NH_2NH_2 \cdot H_2O$, 120–130 °C, 3–4 h (**8a–c**) or r.t., 6 h (**8d**); (c) abs. EtOH, **9a–l**, reflux 1–18 h.

As previously reported, the final reaction proved to be stereoselective and only hydrazones *E* were isolated, as assessed by NMR spectral analyses [34].

2.2. In Vitro Antioxidant Activity (DPPH Assay)

The antioxidant activity of the new synthesized compounds was measured in vitro using the 2,2-diphenyl-1-picrylhydrazyl (DPPH) assay [42,43]. The results were calculated as Trolox equivalent and expressed as percentage of antioxidant activity (AA%) (Table 2). The best AA% values have been obtained for **4b** and **4c** (27.65 and 15.47%, respectively); intermediate activity was shown by **1d**, **1h**, **1i**, **2b**, **2c**, **3c**, and **4a** (AA% range = 4.22–6.12%), while all other tested compounds resulted ineffective.

Table 2. Evaluation of antioxidant activity percent (AA%) using DPPH assay.

Compound	A (517 nm) [a]	DPPH% [b]	AA% [b]
1a	0.917	99.48 ± 0.31	0.30 ± 0.31
1b	0.909	98.93 ± 0.15	1.17 ± 0.15
1c	0.917	99.59 ± 0.08	0.36 ± 0.08
1d	0.881	95.56 ± 0.31	4.22 ± 0.31
1e	0.910	98.83 ± 0.15	1.07 ± 0.15
1f	0.912	99.04 ± 0.15	0.85 ± 0.15
1g	0.909	98.72 ± 0.15	1.17 ± 0.15
1h	0.869	94.59 ± 0.15	5.52 ± 0.15
1i	0.864	93.93 ± 0.08	6.12 ± 0.08
2a	0.900	97.85 ± 0.08	2.21 ± 0.08
2b	0.867	94.48 ± 0.38	5.79 ± 0.38
2c	0.872	94.91 ± 0.23	5.25 ± 0.23
3a	0.914	98.93 ± 0.54	0.68 ± 0.54
3b	0.915	99.37 ± 0.08	0.58 ± 0.08
3c	0.865	94.37 ± 0.46	5.96 ± 0.46
4a	0.873	94.69 ± 0.31	5.09 ± 0.31
4b	0.666	72.08 ± 0.38	27.65 ± 0.38
4c	0.778	84.47 ± 0.08	15.47 ± 0.08
DPPH	0.920	-	-

[a] Absorbance. [b] Mean value ± standard deviation (SD) of two independent experiments (n = 2).

2.3. Inhibiting Effect on Human Platelet Aggregation and ROS Production

As previously reported for compounds **I** and **II**, platelets could be considered inflammatory cells and could represent a simple, economic, and suitable cellular model based on a causal relationship between inflammation and tumorigenesis [34]. Inflammation and thrombosis are two critical, closely interconnected processes in the response to injury and infection. This correlation has long been recognized, particularly in atherosclerotic cardiovascular disease [44] as well in cancer [45].

Oxidative stress has been associated with several pathological conditions (e.g., cancer, diabetes, metabolic disorders, atherosclerosis, and cardiovascular diseases) [46] and plays a significant role in promoting inflammation and platelet activation [47]. Thus, we tested the new 5AP library on human platelets to verify the inhibitory activity on aggregation and ROS production. As reported in Table 3, the newly synthetized compounds affected platelet aggregation and ROS production. Thus, the majority of the tested derivatives displayed $IC_{50} \leq 200$ μM on both tested parameters; **3b** and **3c** showed the higher inhibitory properties against both platelet aggregation and ROS production (IC_{50} values between 113 and 139 μM). It should also be noted that three compounds have intermediate IC_{50} values (around 400 μM), while five are virtually inactive.

Table 3. Inhibitory effect of new APs **1–4** and reference compounds **ASA** (acetylsalicylic acid) and **NAC** (N-acetylcysteine) on platelet aggregation and ROS production on human platelets expressed as IC_{50} (μM) values.

Compound	IC_{50} (μM) [a]	
	Aggregation Inhibition	ROS Production Inhibition
1a	560 ± 27	473 ± 43
1b	137 ± 5	143 ± 12
1c	483 ± 12	451 ± 42
1d	851 ± 17	923 ± 62
1e	953 ± 18	960 ± 32
1f	>1000	>1000
1g	914 ± 22	902 ± 43
1h	187 ± 33	236 ± 47
1i	190 ± 43	240 ± 53
2a	221 ± 26	198 ± 26
2b	334 ± 22	302 ± 36
2c	>1000	>1000
3a	130 ± 18	143 ± 13
3b	113 ± 3	128 ± 5
3c	116 ± 3	139 ± 12
4a	146 ± 24	186 ± 18
4b	178 ± 27	145 ± 28
4c	169 ± 28	205 ± 24
ASA	438 ± 18	n.d.
NAC	n.d.	872 ± 26

[a] Reported data are the mean +/− SD obtained in six different experiments each performed in duplicate. n.d.: not determined.

2.4. Cell Growth Inhibitory Activity

APs **1–4** were tested for anti-proliferative activity on a panel of 60 different cancer cell lines by National Cancer Institute (Developmental Therapeutics Program, Division of Cancer Treatment and Diagnosis, Table 4) [48].

Compounds **2** (3-methyl substituted pyrazoles) and **4** (3-benzylidenecarbohydrazide pyrazoles) did not show a relevant anti-cancer effect, thus indicating that 3-unsubstitued pyrazole scaffold is as key determinant for anti-proliferative activity. Conversely, compounds **1**, close analogues of previous **II**, and derivatives **3**, characterized by a more flexible chain on N1, evidenced a good percentage of cancer cell growth inhibition in different cancer cell lines (Table 4).

Interestingly, among compounds **1**, only derivatives with hindered substituents on catechol portion (i.e., OPh, OCH_2Ar) and more strictly related to previous **I** showed growth percent inhibition values lower than 40% against selected cancer cell lines (**1c** and **1f** on breast cancer cell lines; **1d** on leukemia cell lines and breast cancer cell lines, **1e** on renal cell lines; Table 4). Remarkably, compound **1e** proved to selectively block the growth of renal cancer cell line CAKI-1.

Within series **3**, compounds **3a** and **3c** showed a relevant anti-proliferative activity against different leukemic cell lines.

The significant cell growth inhibitory activity of **1c**, **1d**, **1f,** and **1g** against breast cancer cell lines prompted us to further evaluate (at fixed concentration of 10 μM, MTT assay) their effect against other breast adenocarcinoma cancer cell lines (namely, MCF7, MDA-MB231, and SK-BR3) using Cisplatin as reference compound (Table 5). 5-APs **1c** and **1d** were inactive against all three cell lines, **1f** selectively inhibited SK-BR3 cell lines (65% of cell growth), while **1g** showed remarkable action against all breast cancer cell lines, particularly against SKBR3, evidencing a GI_{50} value lower than reference compound Cisplatin (14.4 μM versus 26 μM).

Table 4. Cell growth percent values of most active 5APS **1–4** on different cancer cell lines at 10 μM concentration. For each compound, only cell lines with a growth percent values ≤ 50% are indicated.

Compound	Cancer Cell Lines		Cell Growth Percent (%)
1c	Leukemia	RPMI-8226	48.0
		SR	44.43
	Colon Cancer	HCT-15	49.2
		KM12	50.97
	Breast Cancer	T-47D	33.11
1d	Leukemia	CCRF-CEM	34.92
		MOLT-4	43.36
		K-562	50.96
		SR	40.25
	Colon Cancer	KM12	44.11
	Breast Cancer	T-47D	25.19
1e	Renal Cancer	CAKI-1	32.41
1f	Leukemia	CCRF-CEM	43.46
		RPMI-8226	50.80
	Breast Cancer	T-47D	35.88
1g	Colon Cancer	HCT-116	49.35
	Ovarian Cancer	OVCAR-3	45.03
	Breast Cancer	HS 578t	43.21
3a	Leukemia	K-562	38.64
		MOLT-4	37.84
		RPMI-8226	45.20
		SR	40.35
	Melanoma	SK-MEL-5	50.43
	Breast Cancer	T-47D	44.38
3c	Leukemia	CCRF-CEM	45.70
		K-562	29.16
		MOLT-4	35.03
		RPMI-8226	46.77
		SR	41.04
	Prostate Cancer	PC-3	48.28

Table 5. Cell growth percent values of **1c**, **1d**, **1f,** and **1g** and Cisplatin, used as reference compound, on three breast cancer cell lines at 10 μM concentration. Data are mean values for three separate experiments. Variation among triplicate samples is less than 10%. For **1g**, GI_{50} values (μM) were also reported.

	1c	1d	1f	1g	Cis-Pt
Breast cancer cell line					
MCF7	>80	>80	>80	52.14%	72.74%
MDA-MB231	>80	>80	>80	55.0%	72.74%
SK-BR3	>80	>80	65.37%	44.78% (GI_{50} = 14.4 ± 0.3 μM)	70.59% (GI_{50} = 25.7 ± 3.3 μM)

2.5. Pharmacokinetic Properties, Druglikness and Toxicity Prediction

To evaluate the pharmaceutical relevance of this new library of 5APs, the pharmacokinetics and drug-likeness properties of all compounds were calculated by SwissADME (Tables S1 and S2, Supporting Information) [49].

Collectively the considered compounds are characterized by eight to twelve rotatable bonds, five to eight H-bond acceptors, three H-bond donors, and TPSA values of 123.99 A^2 except **1a** and **2a** (114.76 A^2), thus supporting a good capacity of all derivatives to permeate lipophilic barriers. In detail, none of the novel 5APs are able to pass brain-blood barrier (BBB), whereas gastrointestinal (GI) absorption is predicted high for derivatives **1a–g**, **2a**,**3a**,

and **4a**. Except for **1i**, all 5APs are predicted to be moderately soluble with a further gain in water solubility for derivatives **3a,b** (ESOL method) [50]. A Lipinski violation (MW > 500 Da) was identified for compounds **1e–i**, **2b**, **2c**, **3c**, **4b**, and **4c**, but no compound showed any pan-assay interference compound (PAINS) alerts. Finally, the presence of a C=N functionality was identified as a limitation, according to the Brenk filter [51].

In addition, the toxicity profiles of all novel compounds were predicted using ProTox webserver (Table S3, Supporting Information) [52,53]. According to the simulation, all APs were predicted to belong to toxicity class 5 (predicted LD_{50} of 4540 mg/kg), with the exception of compounds **1g**, **1i**, and **2a** (predicted LD_{50} = 1000 mg/kg, class 4) and derivative **4c** (LD_{50} = 6000 mg/kg, class 6). No novel derivatives would show any hepatotoxicity, cardiotoxicity, and nephrotoxicity [54], but for most of them (except **1a**, **2c**, and **3a–c**), immunotoxicity (B cell growth inhibition) has been predicted [55]. Finally, no toxicity targets pharmacophores (Novartis off-targets, Adenosine A2a receptor, Adrenergic beta 2 receptor, Androgen receptor, Amine oxidase A, Corticotropin-releasing hormone receptor 1, Dopamine D3 receptor, Estrogen receptor 1, Estrogen receptor 2, Glucocorticoid receptor, Histamine H1 receptor, Nuclear receptor subfamily 1 group I member 2, Opiod receptor kappa 1, Progesterone receptor, Phosphodiesterase 4D, Prostaglandin G/H synthase 1) have been detected.

3. Discussion and Conclusions

The biological results reported here pointed at 5AP scaffold as an interesting chemotype to obtain new potential antioxidant/anti-inflammatory/anti-proliferative agents. In detail, the following SARs have been defined (Figure 3):

(i) The presence of the acylhydrazone moiety at position 3 of the pyrazole core increases the radical scavenging activity (compare **4** with **1–3**);

(ii) The best ROS inhibitors in human platelets are 5APs **3** (particularly **3b** and **3c**, with IC_{50} values of 113–115 μM), characterized in N1 by a more flexible alkyl chain (hydroxyhexyl). Furthermore, the substituents on the cathecol portions of these compounds (difluoromethoxy in *para* position and phenoxy or benzyloxy in *meta* position) are the same of **II**, previously identified as potent ROS inhibitors. In addition, **3c** showed significative anti-cancer profile against different leukemic cell lines. These data confirmed the key role of a flexible hydroxyalkyl chain on N1 position, not only for ROS production inhibition, but also for anti-cancer activity;

(iii) 5APs **1** showed promising anti-proliferative activity, probably related to the chemical similarity of these compounds with previous derivatives **I**. Of note is the fact that **1g** (active against breast cancer cell lines) bears the same substituents on the catechol fragment of its precursor **Ia**.

(iv) Finally, compounds **2**, bearing an additional methyl group on C3 position of pyrazole nucleus, did not show a relevant biological activity, confirming that the increase of steric hindrance in this position is detrimental not only for antioxidant activity and ROS production inhibition in platelets but also for anti-proliferative activity.

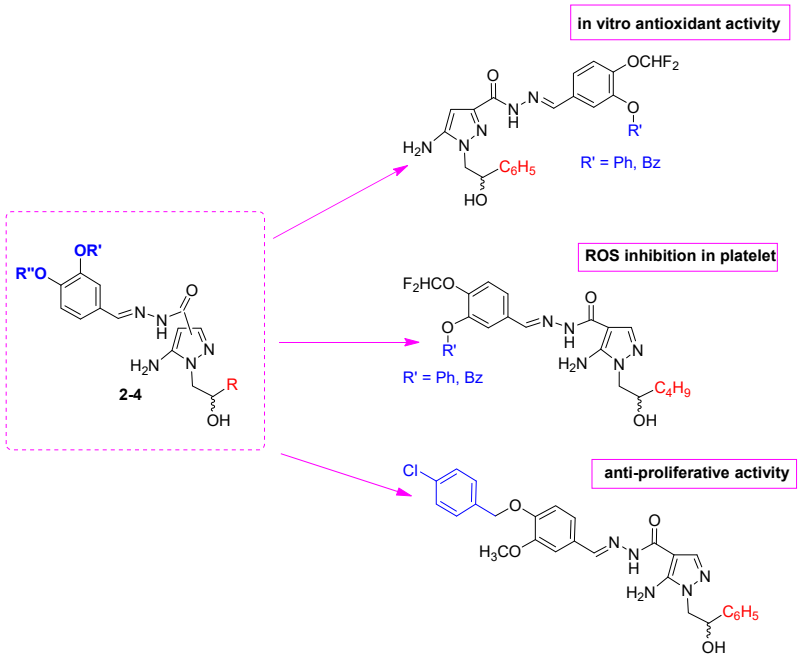

Figure 3. Schematic representation of SARs of novel 5APs here reported.

Collectively, the results here reported extend the SARs on 5AP scaffold, confirming its role as important chemo-type to obtain compounds able to counteract cancer and inflammation.

4. Materials and Methods

4.1. Chemical Part

4.1.1. General Information

Chiminord (Milan, Italy) and Aldrich Chemical (Milan, Italy) purchased all chemicals. Solvents were reagent grade. Unless otherwise stated, all commercial reagents were used without further purification. Organic solutions were dried over anhydrous sodium sulphate. A thin layer chromatography (TLC) system was used for routine monitoring of the course of reactions and confirming the purity of analytical samples. Detection of spots was performed using UV light. Merck silica gel, 230–400 mesh, was used for chromatography. Flash chromatography was performed using Isolera one instrument (Biotage, Uppsala, Sweden) using Silicagel column. Melting points are not "corrected" and were measured with a Buchi M-560 instrument (Buchi instruments, Flawil, Switzerland). NMR spectra were recorded on JEOL JNM-ECZR (400 MHz, Tokyo, Japan) instruments (Figures S1–S42, Supporting Information) using $CDCl_3$ or DMSO-d_6 as solvent; chemical shifts are reported as δ (ppm) and signals were characterized as s (singlet), d (doublet), t (triplet), n t (near triplet), q (quartet), m (multiplet), br s (broad signal); J are reported in Hz.

Elemental analysis was determined with an elemental analyzer EA 1110 (Fison-Instruments, Milan, Italy) and the purity of all synthesized compounds was >95%; products are considered pure when the difference between calculated and found values is ± than 0.4.

4.1.2. Synthesis

Synthesis of compounds **7a–d** and **8b** are yet reported [34,37,38].

Synthesis of Carbohydrazide **8a**, **8c**, and **8d**

Suitable compound **7** (5 mmol) and hydrazine monohydrate (0.25 g, 0.25 mL, 5 mmol) are heated to 120–130 °C for 4 h (**8a** and **8c**) or at room temperature for 6 h (**8d**). After cooling to room temperature, H_2O is added (5 mL) and the white solid obtained is filtered,

washed several times with H_2O, and recrystallized from a mixture of ethanol/methanol (1:2) (**8a**, **8c**) or absolute ethanol (**8d**).

5-Amino-1-(2-hydroxyhexyl)-1H-pyrazole-4-carbohydrazide **8a**. Yield: 78%. M.p.: 140–142 °C. ^{1}H-NMR (400 MHz, $CDCl_3$): δ 0.86 (t, J = 5.4 Hz, 3H, CH_3), 1.15–1.58 (m, 6H, $3CH_2$), 4.56–4.66 (m, 2H, CH_2N pyraz.), 4.92 (br s, 2H, NH_2, exchangeable with D_2O), 5.02 (d, J = 4.4, 1H, OH, exchangeable with D_2O), 5.13–5.18 (m, 1H, *CH*OH), 6.20 (s, 2H, NH_2, exchangeable with D_2O), 7.65 (s, 1H, H-3 pyraz.), 8.97 (br s, 1H, CONH, exchangeable with D_2O). ^{13}C-NMR (101 MHz, $CDCl_3$): δ 164.48, 149,03, 138.30, 97.48, 70.38, 53.18, 35.00, 27.54, 22.74, 14.05. Anal calcd. for $C_{10}H_{19}N_5O_2$. Calcd: %C 49.79, %H 7.94, %N 29.02; found: %C 49.72, %H 7.62, %N 29.30.

5-Amino-1-(2-hydroxy-2-phenylethyl)-3-methyl-1H-pyrazole-4-carbohydrazide **8c**. Yield: 85%. M.p.: 224–226 °C. ^{1}H-NMR (400 MHz, $CDCl_3$): δ 2.24 (s, 3H, CH_3), 3.83–3.94 (m, 2H, CH_2N), 4.28 (br s, 2H, NH_2, exchangeble with D_2O), 4.84–4.88 (m, 1H, C*H*OH), 5.78 (d, J = 4.4, 1H, OH, exchangeble with D_2O), 6.03 (s, 2H, NH_2, exchangeble with D_2O), 7.23–7.48 (m, 5H, 5Ar), 8.02 (s, 1H, CONH, exchangeble with D_2O). ^{13}C-NMR (101 MHz, $CDCl_3$): δ 166.87, 151.19, 150.25, 142.40, 128.56, 128.19, 127.25, 93.34, 73.03, 56.46, 14.93. Anal calcd. for $C_{13}H_{17}N_5O_2$. Calcd: %C 56.71, %H 6.22, %N 25.44; found: %C 56.94, %H 6.02, %N 25.06.

5-Amino-1-(2-hydroxy-2-phenylethyl)-1H-pyrazole-3-carbohydrazide **8d**. Yield: 85%. M.p.: 72–73 °C. ^{1}H-NMR (400 MHz, $CDCl_3$): δ 3.92–4.08 (m, 2H, CH_2N), 4.90–4.94 (m, 1H, C*H*OH), 5.23 (br s., 2H, NH_2, exchangeble with D_2O), 5.30 (d, J = 4.4, 1H, OH, exchangeble with D_2O), 5.66 (s, 1H, H-4 pyraz.), 5.91 (s, 2H, NH_2, exchangeble with D_2O), 7.11–7.54 (m, 5H, 5Ar), 8.01 (br s, 1H, CONH, exchangebles with D_2O). ^{13}C-NMR (101 MHz, $CDCl_3$): δ 162.76, 56.25, 150.62, 145.20, 142.39, 128.56, 128.19, 127.25, 87.47, 72.89. Anal calcd. for $C_{12}H_{15}N_5O_2$. Calcd: %C 55.16, %H 5.79, %N 26.80; found: %C 55.00, %H 5.49, %N 26.46.

Synthesis of Final Compounds **1–4**

To a solution of suitable carbohydrazide **8a–d** (1 mmol) in absolute ethanol (10 mL), the suitable aldehyde **9a–l** (1 mmol), solved in absolute ethanol (2 mL), is added dropwise, then the reaction mixture is heated at reflux for 1–18 h. After cooling to room temperature, the solvent is removed under reduced pressure to obtain yellow/white solids, which are filtered and recrystallized from abs. ethanol (compounds **1**) or diethyl ether (compounds **2–4**).

(E)-5-Amino-1-(2-hydroxy-2-phenylethyl)-N′-(4-methoxybenzylidene)-1H-pyrazole-4-carbohydrazide **1a**. Yield: 61%. M.p.: 233–234 °C. ^{1}H-NMR (400 MHz, $CDCl_3$): δ 3.76 (s, 3H, OCH_3), 3.84–4.13 (m, 2H, CH_2N), 4.85–4.88 (m, 1H, *CH*OH), 5.68 (d, J = 4.6 Hz, 1H, OH, exchangeable with D_2O), 6.12 (s, 2H, NH_2, exchangeable with D_2O), 7.25–7.46 (m, 9H, 5Ar + H-2 Ar + H-3 Ar + H-5 Ar + H-6 Ar), 7.86 (s, 1H, H-3 pyraz.), 8.11 (s, 1H, CH=N), 10.98 (s, 1H, CONH, exchangeable with D_2O). ^{13}C-NMR (101 MHz, $CDCl_3$): δ 164.49, 161.94, 149.28, 148.53, 142.40, 136.23, 128.80, 128.56, 128.19, 127.25, 126.79, 114.41, 113.80, 97.65, 70.60, 55.72, 55.35. Anal calcd. for $C_{20}H_{21}N_5O_3$. Calcd: %C 63.31, %H 5.58, %N 18.46; found: %C 63.38, %H 5.62, %N. 18.22.

(E)-5-Amino-N′-(3,4-dimethoxybenzylidene)-1-(2-hydroxy-2-phenylethyl)-1H-pyrazole-4-carbohydrazide **1b**. Yield: 32%. M.p.: 89–90 °C. ^{1}H-NMR (400 MHz, $CDCl_3$): δ 3.74 (s, 3H, OCH_3), 3.79 (s, 3H, OCH_3), 3.89–4.10 (m, 2H, CH_2N), 4.86–4.89 (m, 1H, *CH*OH), 5.67 (d, J = 4.7 Hz, 1H, OH, exchangeable with D_2O), 6.26 (s, 2H, NH_2, exchangeable with D_2O), 6.87–7.42 (m, 8H, 5Ar + H-2 Ar + H-5 Ar + H-6 Ar), 7.85 (s, 1H, H-3 pyraz.), 8.11 (s, 1H, CH=N), 11.02 (s, 1H, CONH, exchangeable with D_2O). ^{13}C-NMR (101 MHz, $CDCl_3$): δ 160.95, 151.87, 150.32, 149.28, 144.57, 142.40, 136.31, 128.56, 128.19, 127.99, 127.25, 124.16, 111.32, 109.92, 97.65, 70.76, 55.94, 55.93, 55.72. Anal calcd. for $C_{21}H_{23}N_5O_4$. Calcd: %C 61.60, %H 5.66, %N 17.10; found: %C 61.25, %H 5.38, %N 17.14.

(E)-5-Amino-1-(2-hydroxy-2-phenylethyl)-N′-(4-methoxy-3-phenoxybenzylidene)-1H-pyrazole-4-carbohydrazide **1c**. Yield: 32%. M.p.: 190–191 °C. ^{1}H-NMR (400 MHz, $CDCl_3$): δ 3.77 (s, 3H, OCH_3), 3.88–4.07 (m, 2H, CH_2N), 4.83–4.85 (m, 1H, C*H*OH), 5.66 (d, J = 4.7 Hz, 1H,

OH, exchangeable with D_2O), 6.30 (s, 2H, NH_2, exchangeable with D_2O), 6.73–7.49 (m, 13H, 10Ar + H-5 Ar + H-6 Ar + H-2 Ar), 7.77 (s, 1H, H-3 pyraz.), 8.15 (s, 1H, CH=N), 11.01 (s, 1H, CONH, exchangeable with D_2O). ^{13}C NMR (101 MHz, DMSO-d_6): δ 157.89, 152.89, 143.17, 130.41, 128.65, 128.55, 127.92, 126.72, 123.15, 117.08, 72.00, 56.40, 54.46. Anal calcd. for $C_{26}H_{25}N_5O_4$. Calcd: %C 66.23, %H 5.34, %N 14.85; found: %C 65.86, %H 5.31, %N 14.38.

(E)-5-Amino-N′-(3-(benzyloxy)-4-methoxybenzylidene)-1-(2-hydroxy-2-phenylethyl)-1H-pyrazole -4-carbohydrazide **1d**. Yield: 62%. M.p.: 161–163 °C. ^{1}H-NMR (400 MHz, $CDCl_3$): δ 3.77 (s, 3H, OCH_3), 3.91–4.09 (m, 2H, CH_2N), 4.89–4.90 (m, 1H, *CH*OH), 5.10 (s, 2H, CH_2O), 5.68 (d, J = 4.6 Hz, 1H, OH, exchangeable with D_2O), 6.39 (s, 2H, NH_2, exchangeable with D_2O), 6.92–7.60 (m, 13H, 10Ar + H-5 Ar + H-6 Ar + H-2 Ar), 7.84 (s, 1H, H-3 pyraz.), 8.10 (s, 1H, CH=N), 10.99 (s, 1H, CONH, exchangeable with D_2O). ^{13}C-NMR (101 MHz, $CDCl_3$): δ 160.95, 152.83, 149.28, 149.26, 144.57, 142.40, 137.41, 135.44, 128.56, 128.50, 128.19, 128.16, 128.12, 127.71, 127.25, 124.42, 112.85, 112.10, 97.65, 71.88, 71.05, 56.07, 55.72. Anal calcd. for $C_{27}H_{27}N_5O_4$. Calcd: %C 66.79, %H 5.61, %N 14.42; found: %C 66.66, %H 5.77, %N 14.48.

(E)-5-Amino-N′-(4-((4-fluorobenzyl)oxy)-3-methoxybenzylidene)-1-(2-hydroxy-2-phenylethyl)-1H-pyrazole-4-carbohydrazide **1e**. Yield: 75%. M.p.: 136–137 °C. ^{1}H-NMR (400 MHz, $CDCl_3$): δ 3.78 (s, 3H, OCH_3), 3.91–4.12 (m, 2H, CH_2N), 4.91–4.93 (m, 1H, *CH*OH), 5.04 (s, 2H, CH_2O), 5.69 (d, J = 4.6 Hz, 1H, OH, exchangeable with D_2O), 6.28 (s, 2H, NH_2, exchangeable with D_2O), 7.00–7.56 (m, 12H, 9Ar + H-5 Ar + H-6 Ar + H-2 Ar), 7.86 (s, 1H, H-3 pyraz.), 8.10 (s, 1H, CH=N), 11.04 (s, 1H, CONH, exchangeable with D_2O). ^{13}C NMR (101 MHz, DMSO-d_6): δ 163.59, 161.17, 149.89, 149.63, 143.19, 133.63, 133.60, 130.74, 130.65, 128.67, 128.41, 127.94, 126.73, 115.92, 115.71, 113.81, 72.04, 69.68, 55.94, 54.51, 40.50. Anal calcd. for $C_{27}H_{26}N_5O_4F$. Calcd: %C 64.40, % H 5.20, %N 13.91; found: %C 64.55, %H 5.37, %N 13.51.

(E)-5-Amino-N′-(4-((3-fluorobenzyl)oxy)-3-methoxybenzylidene)-1-(2-hydroxy-2-phenylethyl)-1H-pyrazole-4-carbohydrazide **1f**. Yield: 64%. M.p.: 123–125 °C. ^{1}H-NMR (400 MHz, $CDCl_3$): δ 3.81 (s, 3H, OCH_3), 3.90–4.12 (m, 2H, CH_2N), 4.89–4.91 (m, 1H, *CH*OH), 5.12 (s, 2H, CH_2O), 5.68 (d, J = 4.6 Hz, 1H, OH, exchangeable with D_2O), 6.31 (s, 2H, NH_2, exchangeable with D_2O), 6.96–7.48 (m, 12H, 9Ar + H-5 Ar + H-6 Ar + H-2 Ar), 7.86 (s, 1H, H-3 pyraz.), 8.10 (s, 1H, CH=N), 11.03 (s, 1H, CONH, exchangeable with D_2O). ^{13}C NMR (101 MHz, DMSO-d_6): δ 163.93, 161.51, 149.90, 149.47, 143.19, 140.40, 140.32, 131.09, 131.01, 128.67, 128.55, 127.94, 126.73, 124.23, 124.20, 115.33, 115.12, 115.00, 114.78, 113.87, 72.03, 69.55, 55.99, 54.50, 40.70, 40.49. Anal calcd. for $C_{27}H_{26}N_5O_4F$. Calcd: %C 64.40, %H 5.20, %N 13.91; found: %C 64.82, %H 5.16, %N 13.78.

(E)-5-Amino-N′-(4-((4-chlorobenzyl)oxy)-3-methoxybenzylidene)-1-(2-hydroxy-2-phenylethyl)-1H-pyrazole-4-carbohydrazide **1g**. Yield: 48%. M.p.: 120–123 °C. ^{1}H-NMR (400 MHz, $CDCl_3$): δ 3.79 (s, 3H, OCH_3), 3.85–4.13 (m, 2H, CH_2N), 4.88–4.91 (m, 1H, *CH*OH), 5.15 (s, 2H, CH_2O), 5.67 (d, J = 4.4 Hz, 1H, OH, exchangeable with D_2O), 6.36 (s, 2H, NH_2, exchangeable with D_2O), 6.99–7.49 (m, 12H, 9Ar + H-5 Ar + H-6 Ar + H-2 Ar), 7.77 (s, 1H, H-3 pyraz.), 8.12 (s, 1H, CH=N), 11.02 (s, 1H, CONH, exchangeable with D_2O). ^{13}C NMR (101 MHz, DMSO-d_6): δ 149.89, 149.51, 143.19, 136.47, 133.05, 130.19, 129.01, 128.67, 128.49, 127.94, 126.73, 72.03, 69.53, 55.97, 54.50, 40.50. Anal calcd. for $C_{27}H_{26}N_5O_4Cl$. Calcd: %C 62.37, %H 5.04, %N 13.47; found: %C 62.39, %H 5.28, %N 13.86.

(E)-5-Amino-N′-(4-(difluoromethoxy)-3-((3-fluorobenzyl)oxy)benzylidene)-1-(2-hydroxy-2-phenylethyl)- 1H-pyrazole-4-carbohydrazide **1h**. Yield: 82%. M.p.: 148–153 °C. ^{1}H-NMR (400 MHz, $CDCl_3$): δ 3.90–4.12 (m, 2H, CH_2N), 4.85–4.87 (m, 1H, CHOH), 5.23 (s, 2H, CH_2O), 5.68 (d, J =4.4, 1H, OH, exchangeable with D_2O), 6.37 (s, 2H, NH_2, exchangeable with D_2O), 7.15 (t, J = 70 Hz, 1H, $OCHF_2$), 7.21–7.50 (m, 12H, 9Ar + H-5 Ar + H-6 Ar + H-2 Ar), 7.96 (s, 1H, H-3 pyraz.), 8.21 (s, 1H, CH=N), 11.18 (s, 1H, CONH, exchangeable with D_2O). ^{13}C NMR (101 MHz, DMSO-d_6): δ 163.98, 161.56, 150.30, 143.17, 141.20, 139.98, 139.91, 133.76, 131.17, 131.08, 128.67, 127.94, 126.74, 123.97, 122.21, 119.88, 117.31, 115.44, 115.23, 114.74, 114.52, 72.03, 69.63, 54.49. Anal calcd. for $C_{27}H_{24}N_5O_4F_3$. Calcd: %C 60.11, %H 4.48, %N 12.98; found: %C 60.23, %H 4.60, %N 13.12.

(E)-5-Amino-N′-(3-((4-chlorobenzyl)oxy)-4-(difluoromethoxy)benzylidene)-1-(2-hydroxy-2-phenylethyl)-1H-pyrazole-4-carbohydrazide **1i**. Yield: 81%. M.p.: 106–108 °C. ^{1}H-NMR (400 MHz, $CDCl_3$): δ 3.83–4.14 (m, 2H, CH_2N), 4.87–4.90 (m, 1H, CHOH), 5.23 (s, 2H, CH_2O), 5.68 (d, J = 4.4, 1H, OH, exchangeable with D_2O), 6.32 (s, 2H, NH_2, exchangeable with D_2O), 7.13 (t, J = 70 Hz, 1H, $OCHF_2$), 7.21–7.53 (m, 12H, 9Ar + H-5 Ar + H-6 Ar + H-2 Ar), 7.94 (s, 1H, H-3 pyraz.), 8.18 (s, 1H, CH=N), 11.18 (s, 1H, CONH, exchangeable with D_2O). ^{13}C NMR (101 MHz, DMSO-d_6): δ 150.28, 143.17, 141.23, 136.07, 133.68, 133.17, 130.98, 129.98, 129.11, 128.90, 128.67, 127.95, 126.75, 122.07, 119.83, 117.26, 114.69, 112.19, 72.04, 69.66, 54.49, 40.70, 38.25. Anal calcd. for $C_{27}H_{24}N_5O_4ClF_2$. Calcd: %C 58.33, %H 4.35, %N 12.60; found: %C 58.10, %H 4.33, %N 12.35.

(E)-5-Amino-N′-(4-(difluoromethoxy)-3-methoxybenzylidene)-1-(2-hydroxy-2-phenylethyl)-3-methyl-1H-pyrazole-4-carbohydrazide **2a**. Yield: 46%. M.p.: 193–195 °C. ^{1}H-NMR (400 MHz, $CDCl_3$): δ 2.31 (s, 3H, CH_3), 3.65–4.12 (m, 5H, CH_2N + OCH_3), 4.83–4.86 (m, 1H, CHOH), 5.70 (d, J = 4.6 Hz, 1H, OH, exchangeable with D_2O), 6.05 (s, 2H, NH_2, exchangeable with D_2O), 7.28 (t, J = 70, 1H, $OCHF_2$), 7.37–7.67 (m, 8H, 5 Ar + H-5 Ar + H-6 Ar + H-2 Ar), 8.25 (s, 1H, CH=N), 11.42 (s, 1H, CONH, exchangeable with D_2O). ^{13}C-NMR (101 MHz, $CDCl_3$): δ 166.24, 151.94, 150.72, 149.40, 144.53, 144.45, 142.40, 128.30, 128.19, 127.25, 121.90, 118.71, 118.69, 117.87, 115.77, 113.66, 110.53, 93.67, 73.03, 56.45, 56.23, 14.93. Anal calcd. for $C_{22}H_{23}N_5O_4F_2$. Calcd: %C 57.51, %H 5.05, %N 15.24; found: %C 57.31, %H 5.26, %N 15.64.

(E)-5-Amino-N′-(4-(difluoromethoxy)-3-phenoxybenzylidene)-1-(2-hydroxy-2-phenylethyl)-3-methyl-1H-pyrazole-4-carbohydrazide **2b**. Yield: 25%. M.p.: 203–206 °C. ^{1}H-NMR (400 MHz, $CDCl_3$): δ 2.51 (s, 3H, CH_3), 3.71–4.10 (m, 2H, CH_2N), 4.84–4.85 (m, 1H, CHOH), 5.71 (d, J = 4.6 Hz, 1H, OH, exchangeable with D_2O), 5.95 (s, 2H, NH_2, exchangeable with D_2O), 6.94–7.53 (m, 14H, 10Ar + H-5 Ar + H-6 Ar + H-2 Ar + $OCHF_2$), 8.21 (s, 1H, CH=N), 10.32 (s, 1H, CONH, exchangeable with D_2O). ^{13}C-NMR (101 MHz, $CDCl_3$): δ 166.24, 156.83, 152.85, 150.72, 147.66, 145.72, 144.77, 142.40, 130.02, 128.19, 127.25, 124.60, 122.31, 122.17, 120.07, 118.73, 117.96, 115.73, 115.71, 115.69, 114.87, 92.84, 74.52, 54.27, 16.24. Anal calcd. for $C_{27}H_{25}N_5O_4F_2$. Calcd: %C 62.18, %H 4.83, %N 13.43; found: %C 62.37, %H 4.25, %N 13.34.

(E)-5-Amino-N′-(3-(benzyloxy)-4-(difluoromethoxy)benzylidene)-1-(2-hydroxy-2-phenylethyl)-3-methyl-1H-pyrazole-4-carbohydrazide **2c**. Yield: 75%. M.p.: 188–190 °C. ^{1}H-NMR (400 MHz, $CDCl_3$): δ 2.29 (s, 3H, CH_3), 3.73–4.15 (m, 2H, CH_2N), 4.79–4.82 (m, 1H, CHOH), 5.21 (s, 2H, CH_2O), 5.71 (d, J =4.4, 1H, OH, exchangeable with D_2O), 6.03 (s, 2H, NH_2, exchangeable with D_2O), 7.17 (t, J = 70 Hz, 1H, $OCHF_2$), 7.30–7.63 (m, 13H, 10Ar + H-5 Ar + H-6 Ar + H-2 Ar), 8.22 (s, 1H, CH=N), 10.42 (s, 1H, CONH, exchangeable with D_2O). ^{13}C-NMR (101 MHz, $CDCl_3$): δ 166.24, 154.48, 150.58, 150.56, 145.94, 144.67, 142.40, 137.49, 128.56, 128.50, 128.22, 128.19, 128.16, 127.71, 127.25, 122.14, 119.79, 117.68, 115.58, 112.92, 112.89, 112.87, 111.68, 95.24, 72.49, 71.24, 54.32, 16.33. Anal calcd. for $C_{28}H_{27}N_5O_4F_2$. Calcd: %C 62.80, %H 5.08, %N 13.08; found: %C 62.72, %H 5.18, %N 13.51.

(E)-5-Amino-N′-(4-(difluoromethoxy)-3-methoxybenzylidene)-1-(2-hydroxyhexyl)-1H-pyrazole-4-carbohydrazide **3a**. Yield: 52%. M.p.: 164–165 °C. ^{1}H-NMR (400 MHz, $CDCl_3$): δ 0.85 (s, 3H, CH_3), 1.07–1.48 (m, 6H, $3CH_2$), 3.64–4.03 (m, 5H, OCH_3 + CH_2N), 4.93–4.97 (s, 1H, C*H*OH), 5.67 (d, J = 4.5 Hz, 1H, OH, exchangeable with D_2O), 6.34 (s, 2H, NH_2, exchangeable with D_2O), 7.12 (t, J = 67 Hz, 1H, $OCHF_2$), 7.40–7.54 (m, 3H, H-5 Ar + H-6 Ar + H-2 Ar), 7.99 (s, 1H, H-3 pyraz.), 8.18 (s, 1H, CH=N), 11.22 (s, 1H, CONH exchangeable with D_2O). ^{13}C-NMR (101 MHz, $CDCl_3$): δ 158.95, 151.94, 149.02, 144.53, 135.49, 128.30, 121.90, 118.69, 115.77, 113.66, 110.53, 97.46, 70.38, 56.23, 55.36, 32.62, 27.54, 22.74, 16.41. Anal calcd. for $C_{19}H_{25}N_5O_4F_2$. Calcd: %C 53.64, %H 5.92, %N 16.46; found: %C 53.75, %H 5.81, %N 16.36.

(E)-5-Amino-N′-(4-(difluoromethoxy)-3-phenoxybenzylidene)-1-(2-hydroxyhexyl)-1H-pyrazole-4-carbohydrazide **3b**. Yield: 73%. M.p.: 140–141 °C. ^{1}H-NMR (400 MHz, $CDCl_3$): δ 0.86 (t, 3H, CH_3), 1.14–1.52 (m, 6H, $3CH_2$), 3.65–3.97 (m, 2H, CH_2N), 4.92–4.94 (m, 1H, C*H*OH), 6.01 (d, J = 4.4 Hz, 1H, OH, exchangeable with D_2O), 6.29 (s, 2H, NH_2, exchangeable with D_2O), 6.83 (t, J = 67 Hz, 1H, $OCHF_2$), 7.08–7.63 (m, 8H, 5 Ar + H-5 Ar + H-6 Ar + H-2 Ar),

7.79 (s, 1H, H-3 pyraz.), 8.15 (s, 1H, CH=N), 11.18 (s, 1H, CONH, exchangeable with D_2O). ^{13}C-NMR (101 MHz, $CDCl_3$): δ 165.06, 156.83, 149.02, 147.65, 145.13, 145.08, 144.73, 134.57, 130.02, 128.30, 124.60, 122.31, 118.73, 117.87, 115.76, 114.87, 113.66, 97.46, 70.38, 53.17, 32.77, 27.54, 24.62, 18.06. Anal calcd. for $C_{24}H_{27}N_5O_4F_2$. Calcd: %C 59.13, %H 5.58, %N 14.37; found: %C 59.59, %H 5.46, %N 14.69.

(E)-5-Amino-N′-(3-(benzyloxy)-4-(difluoromethoxy)benzylidene)-1-(2-hydroxyhexyl)-1H-pyrazole-4-carbohydrazide **3c**. Yield: 52%. M.p.: 129–131 °C. ^{1}H-NMR (400 MHz, $CDCl_3$): δ 0.84 (t, J = 5.6 Hz, 3H, CH_3), 1.18–1.65 (m, 6H, $3CH_2$), 3.65–3.99 (m, 2H, CH_2N), 4.85–4.86 (m, 1H, *CH*OH), 5.23 (s, 2H, CH_2O), 6.03 (d, J = 4.4 Hz, 1H, OH, exchangeable with D_2O), 6.35 (s, 2H, NH_2, exchangeable with D_2O), 7.01 (t, J = 67 Hz, 1H, $OCHF_2$), 7.15–7.63 (m, 8H, 5 Ar + H-5 Ar + H-6 Ar + H-2 Ar), 7.97 (s, 1H, H-3 pyraz.), 8.10 (s, 1H, CH=N), 11.22 (s, 1H, CONH, exchangeable with D_2O). ^{13}C-NMR (101 MHz, $CDCl_3$): δ 162.95, 150.55, 149.02, 144.54, 137.49, 135.36, 128.22, 128.16, 127.71, 122.14, 118.44, 118.42, 116.84, 114.74, 112.63, 111.68, 95.84, 71.24, 70.38, 53.17, 31.77, 27.54, 24.31, 18.41. Anal calcd. for $C_{25}H_{29}N_5O_4F_2$. Calcd: %C 59.87, %H 5.83, %N 13.96; found: %C 59.59, %H 5.77, %N 14.10.

(E)-5-Amino-N′-(4-(difluoromethoxy)-3-methoxybenzylidene)-1-(2-hydroxy-2-phenylethyl)-1H-pyrazole-3-carbohydrazide **4a**. Yield: 54%. M.p.: 196–197 °C. ^{1}H-NMR (400 MHz, $CDCl_3$): δ 3.86–3.94 (m, 2H, CH_2N), 3.97 (s, 3H, OCH_3), 4.52 (d, J = 4.4 Hz, 1H, OH, exchangeable with D_2O), 5.10–5.13 (m, 1H, C*H*OH), 5.69 (s, 2H, NH_2, exchangeable with D_2O), 5.74 (s, 1H, H-4 pyraz.), 7.04 (t, J = 70 Hz, 1H, OCHF2), 7.10–7.51 (m, 8H, 5Ar + H-5 Ar + H-6 Ar + H-2 Ar), 8.55 (s, 1H, CH=N), 11.78 (s, 1H, CONH, exchangeable with D_2O). ^{13}C NMR (101 MHz, DMSO-d_6): δ 166.71, 165.11, 150.37, 150.03, 137.50, 136.45, 97.39, 95.92, 69.85, 53.18, 34.39, 27.68, 22.69, 14.51. Anal calcd. for $C_{21}H_{21}N_5O_4F_2$. Calcd: %C 56.60, %H 4.70, %N 15.72; found: %C 56.69, %H 4.42, %N 15.69.

(E)-5-Amino-N′-(4-(difluoromethoxy)-3-phenoxybenzylidene)-1-(2-hydroxy-2-phenylethyl)-1H-pyrazole-3-carbohydrazide **4b**. Yield: 59%. M.p.: 195–196 °C. ^{1}H-NMR (400 MHz, $CDCl_3$): δ 3.92–4.08 (m, 2H, CH_2N), 4.96–4.98 (m, 1H, C*H*OH), 5.33 (d, J = 4.4 Hz, 1H, OH, exchangeable with D_2O), 5.43 (s, 2H, NH_2, exchangeable with D_2O), 5.75 (s, 1H, H-4 pyraz.), 6.92–7.50 (m, 14H, 10Ar + H-5 Ar + H-6 Ar + H-2 Ar + $OCHF_2$), 8.40 (s, 1H, CH=N), 11.41 (s, 1H, CONH, exchangeable with D_2O). ^{13}C-NMR (101 MHz, $CDCl_3$): δ 162.64, 156.83, 151.88, 150.61, 145.08, 144.66, 142.39, 140.61, 130.02, 128.56, 128.32, 128.19, 127.25, 124.60, 122.31, 121.36, 119.25, 118.73, 117.15, 115.73, 115.70, 115.68, 114.87, 87.65, 71.77, 57.42. Anal calcd. for $C_{26}H_{23}N_5O_4F_2$. Calcd: %C 61.53, %H 4.57, %N 13.80; found: %C 61.63, %H 4.95, %N 13.65.

(E)-5-Amino-N′-(3-(benzyloxy)-4-(difluoromethoxy)benzylidene)-1-(2-hydroxy-2-phenylethyl)-1H-pyrazole-3-carbohydrazide **4c**. Yield: 15%. M.p.: 136–137 °C. ^{1}H-NMR (400 MHz, $CDCl_3$): δ 4.00–4.14 (m, 2H, CH_2N), 4.98–5.01 (m, 1H, C*H*OH), 5.17 (s, 2H, CH_2O), 5.36 (d, J = 4.4 Hz, 1H, OH, exchangeable with D_2O), 5.75 (s, 2H, NH_2, exchangeable with D_2O), 5.81 (s, 1H, H-4 pyraz.), 7.02 (t, J = 70 Hz, 1H, $OCHF_2$), 7.22–7.53 (m, 13H, 10Ar + H-5 Ar + H-6 Ar + H-2 Ar), 8.43 (s, 1H, CH=N), 11.44 (s, 1H, CONH, exchangeable with D_2O). ^{13}C-NMR (101 MHz, $CDCl_3$): δ 162.95, 153.71, 153.70, 150.61, 144.49, 144.43, 144.36, 142.39, 140.74, 137.49, 128.50, 128.19, 128.18, 128.16, 127.71, 127.25, 122.14, 120.67, 118.57, 116.46, 112.90, 112.88, 111.68, 86.98, 73.64, 71.24, 57.37. Anal calcd. for $C_{27}H_{25}N_5O_4F_2$. Calcd: %C 62.18, %H 4.83, %N 13.43; found: %C 62.15, %H 4.40, %N 13.01.

4.2. In Vitro Antioxidant Activity (DPPH Assay)

The antioxidant activity was measured using the DPPH antioxidant assay. The assay is based on the bleaching rate of the stable radical DPPH [56]. Briefly, ca 3 mg of single compound was dissolved with methanol, then 0.1 mL of this solution was mixed with 3.9 mL of DPPH methanol solution (65 μM). Absorbance was measured at 517 nm after reacting for 30 min in the dark. Linear calibration curve was obtained using Trolox standards (range between 20 to 200 mg/L, R2 = 0.9988). The result was calculated as Trolox equivalents in

mg/L and the percentage of antioxidant activity (AA%) was calculated from the ratio of decreasing absorbance of sample solution (A0 − As) to absorbance of blank DPPH solution (A0), as expressed in Equation (1) [57].

$$AA\% = [(A0 - As)/A0] \times 100 \quad (1)$$

4.3. Human Platelet Assays

4.3.1. Material

2′,7′-Dichlorofluorescein diacetate (DCFH-DA) and thrombin were purchased from Sigma-Aldrich (St. Louis, MI, USA)/Merck Millipore (Burlington, VT, USA).

4.3.2. Blood Collection and Preparative Procedures

Washed platelets were prepared from freshly drawn venous blood obtained from healthy volunteers at the Centro Trasfusionale, Ospedale San Martino in Genoa. Donors declare that they have not taken any drugs known to interfere with platelet function for at least two weeks prior to blood collection and gave their informed consent. Blood was collected into anticoagulant solution containing 130 mM aqueous trisodium citrate (9:1). Whole blood is centrifuged at 100× *g* for 20 min to obtain platelet-rich plasma (PRP) that is further centrifuged at 1100× *g* for 15 min. The obtained pellet is washed once with an acidic solution containing 75 mM trisodium citrate, 42 mM citric acid, and 136 mM glucose (pH 5.2) and then resuspended in a pH 7.4 Hepes buffer solution (145 mM NaCl, 5 mM KCl, 1 mM $MgSO_4$, 10 mM glucose, and 10 mM HEPES).

IC_{50} values reported represent the molar concentration of a compound required to inhibit 50% of the maximal effect induced by thrombin. The percentage of inhibition is calculated by comparing the inhibition of the maximal effect measured in the presence of the test compound with that measured in a control sample containing saline, under the same experimental conditions.

4.3.3. ROS Assay

ROS production was measured by the ROS-sensitive probe DCFH-DA, which, upon oxidation, forms the fluorescent compound DCF. The DCF formed by ROS is trapped inside the cells, allowing for the quantification of ROS levels [58]. Washed platelets (1.0×10^8/mL) were preincubated with either saline or test compounds for 15 min at 37 °C. Platelets were then stimulated by 0.1 U/mL thrombin for 15 min at 37 °C. After stimulation, the incubation was stopped by cooling in an ice bath; the samples were immediately analyzed using a flow cytometer (Merck Millipore Bioscience Guava easyCyte flow cytometer). IC_{50} values were calculated as described above.

4.3.4. Platelet Aggregation

Born's method [59] is a well-established technique for studying platelet aggregation in response to various stimuli and it provides valuable information about the ability of compounds to modulate platelet function.

Washed platelets (3.0×10^8/mL) were preincubated for 3 min at 37 °C with either saline or test compounds and then stimulated by 0.1 U/mL thrombin. In a BioData Aggregometer (Bio-Data Corporation, Horsham, PA, USA), platelet aggregation is quantified by measuring the light transmission over 6 min at 37 °C. IC_{50} values were calculated as above reported.

4.4. Cell Growth Inibitory activity

1c, **1d**, **1f**, and **1g** were tested at a fixed concentration of 10 μM against three different breast cancer cell lines (namely, MCF7, MDA-MB231, SK-BR3) using Cisplatin (Cis-Pt) as reference compound. Cisplatin was kindly provided by the pharmacy (UFA-Unità Farmaci Antiblastici) of the IRCCS Ospedale Policlinico San Martino.

MTT Assay

To perform MTT assay, SK-BR3 (breast adenocarcinoma, Biologic Bank and Cell Factory, IRCCS Policlinico San Martino, Genoa, Italy), MCF-7 (breast adenocarcinoma, Biologic Bank and Cell Factory, IRCCS Policlinico San Martino, Genoa, Italy), and MDA-MB231 (breast adenocarcinoma, Biologic Bank and Cell Factory, IRCCS Policlinico San Martino, Genoa, Italy) cell lines were cultured in Dulbecco's Modified Eagle Medium (DMEM) added to 10% Fetal bovine serum (FBS), 2 mM Glutamine, and 1% penstrep. Reagents were acquired from EuroClone (Milan, Italy) and incubated in a humidified environment at 37 °C with 5% CO_2. All chemical compounds (**1c**, **1d**, **1f**, and **1g** and Cisplatin, used as reference compound) were dissolved in DMSO to give a 10 mM stock solution. Then, after an intermediate dilution in growth medium, they were added to the cultured cells at a final working concentration of 10 μM and incubated for 48 h. At the end of the incubation, 30 μL of MTT (3-(4,5-dimethyl-2-thiazolyl)-2,5-diphenyl-2H-tetrazolium bromide) at a concentration of 2 mg/mL in PBS, were added in each well and incubated 4 h. Finally, the supernatants were removed and 100 μL/well of DMSO were added to each well to dissolve the Formazan precipitates. After 20 min, the results were read at λ = 570 nm. Results are expressed as a percentage of the control samples, where cells have been treated with the same amount of DMSO but without any chemical compound. The assay was repeated three times, and a single compound was tested six times. Means and standard deviations were calculated.

The GI_{50} values were calculated based on single concentration-response curves. Each experiment was repeated three times.

Supplementary Materials: The following supporting information can be downloaded at: https://www.mdpi.com/article/10.3390/molecules29102298/s1, Table S1. Predicted pharmacokinetics and drug-like properties of compounds **1a-i**. Table S2. Predicted pharmacokinetics and drug-like properties of compounds **2a–c**, **3a–c**, **4a–c**. Table S3. Predicted toxicity of compounds **1a–i, 2a–c**, **3a–c**, **4a–c**. Figures S1–S42: ^{1}H NMR (400 MHz) and ^{13}C NMR (101 MHz) of compounds **8a**,**8c**,**8d** and **1–4**.

Author Contributions: Writing and conceptualization, C.B.; synthesis of compounds, F.R., B.T.; MTT and cell biology, M.P., E.I., C.R.; platelet aggregation and antioxidant inhibitory activity, M.G.S.; DPPH test E.R., D.C., C.V.; statistical analysis and in silico pharmacokinetics, drug-likeness, and toxicity properties, A.S. All authors have read and agreed to the published version of the manuscript.

Funding: E.I.: C.R., M.P. acknowledge the support of the Italian Minister of Health (Ricerca Corrente).

Institutional Review Board Statement: Since blood for the experiments is collected during the voluntary blood donation in the transfusion center of the Hospital, under the Italian legislation it's not necessary to obtain the Ethics Commission Authorization. Donors are healthy subjects who have not undergone any treatment.

Informed Consent Statement: Informed consent was obtained from all subjects involved in the study.

Data Availability Statement: The data presented in this study are available in article and Supplementary Materials.

Acknowledgments: We thank M. Anzaldi and R. Raggio for recording elemental analysis, ^{1}H and ^{13} C spectra. We thank Developmental Therapeutics Program, Division of Cancer Treatment and Diagnosis, National Cancer Institute (NCI, http://dtp.cancer.gov Accessed on 1 May 2024) for cell growth inhibitory activityevaluation.

Conflicts of Interest: The authors declare no conflicts of interest.

References

1. Ebenezer, O.; Shapi, M.; Tuszynski, J.A. A Review of the Recent Development in the Synthesis and Biological Evaluations of Pyrazole Derivatives. *Biomedicines* **2022**, *10*, 1124–1180. [CrossRef]
2. Karrouchi, K.; Radi, S.; Ramli, Y.; Taoufik, J.; Mabkhot, Y.N.; Al-aizari, F.A.; Ansar, M. Synthesis and Pharmacological Activities of Pyrazole Derivatives: A Review. *Molecules* **2018**, *23*, 134–219. [CrossRef]
3. Karati, D.; Mahadik, K.R.; Kumar, D. Pyrazole Scaffolds: Centrality in Anti-Inflammatory and Antiviral Drug Design. *Med. Chem.* **2022**, *18*, 1060–1072. [CrossRef]

4. Karati, D.; Mahadik, K.R.; Trivedi, P.; Kumar, D. A Molecular Insight into Pyrazole Congeners as Antimicrobial, Anticancer, and Antimalarial Agents. *Med. Chem.* **2022**, *18*, 1044–1059. [CrossRef]
5. Ansari, A.; Ali, A.; Asif, M. Biologically active pyrazole derivatives. *New J. Chem.* **2017**, *41*, 16–41. [CrossRef]
6. Li, M.; Zhao, B.X. Progress of the synthesis of condensed pyrazole derivatives (from 2010 to mid-2013). *Eur. J. Med. Chem* **2014**, *85*, 311–340. [CrossRef]
7. Dadiboyena, S.; Nefzi, A. Synthesis of functionalized tetrasubstituted pyrazolyl heterocycles--a review. *Eur. J. Med. Chem.* **2011**, *46*, 5258–5275. [CrossRef]
8. Abu-Hashem, A.A.; Aly, A.S. Synthesis of New Pyrazole, Triazole, Thiazolidine, -Pyrimido [4,5-b] quinoline derivatives with Potential Antitumor Activity. *Arch. Pharm. Res.* **2012**, *35*, 437–445. [CrossRef]
9. Abu-Hashem, A. Synthesis of new pyrazoles, oxadiazoles, triazoles, pyrrolotriazines and pyrrolotriazepines as potential cytotoxic agents. *J. Heter. Chem.* **2021**, *58*, 805–821. [CrossRef]
10. Silva, V.L.; Silva, A.M.S. Special Issue "Recent Advances in the Synthesis, Functionalization and Applications of Pyrazole-Type Compounds". *Molecules* **2021**, *26*, 4989. [CrossRef] [PubMed]
11. Silva, V.L.M.; Silva, A.M.S. Special Issue Recent Advances in the Synthesis, Functionalization and Applications of Pyrazole-Type Compounds II. *Molecules* **2023**, *28*, 5873. [CrossRef]
12. Lusardi, M.; Spallarossa, A.; Brullo, C. Amino-Pyrazoles in Medicinal Chemistry: A Review. *IJMS* **2023**, *24*, 7834. [CrossRef]
13. Bennani, F.E.; Doudach, L.; Cherrah, Y.; Ramli, Y.; Karrouchi, K.; Ansar, M.; Faouzi, M.E.A. Overview of recent developments of pyrazole derivatives as an anticancer agent in different cell line. *Bioorg. Chem.* **2020**, *97*, 103470. [CrossRef]
14. Küçükgüzel, Ş.G.; Şenkardeş, S. Recent advances in bioactive pyrazoles. *Eur. J. Med. Chem.* **2015**, *97*, 786–815. [CrossRef]
15. Bekhit, A.A.; Hymete, A.; El-Din A Bekhit, A.; Damtew, A.; Aboul-Enein, H.Y. Pyrazoles as promising scaffold for the synthesis of anti-inflammatory and/or antimicrobial agent: A review. *Mini Rev. Med. Chem.* **2010**, *10*, 1014–1033. [CrossRef]
16. Bennani, F.E.; Doudach, L.; El Rhayam, Y.; Karrouchi, K.; Cherrah, Y.; Tarib, A.; Ansar, M.; Faouzi, M.E.A. Identification of the new progress on Pyrazole Derivatives Molecules as Antimicrobial and Antifungal Agents. *West Afr. J. Med.* **2022**, *39*, 1217–1244.
17. Anwara, H.F.; Mohamed, H.E. Recent developments in aminopyrazole chemistry. *ARKIVOC* **2009**, 198–250. Available online: https://www.arkat-usa.org/get-file/29257/ (accessed on 8 May 2024). [CrossRef]
18. Abu Elmaati, T.M.; El-Taweel, F.M. New Trends in the Chemistry of 5-Aminopyrazoles. *J. Heterocycl. Chem.* **2004**, *41*, 109–134. [CrossRef]
19. Goldstein, D.M.; Alfredson, T.; Bertrand, J.; Browner, M.F.; Clifford, K.; Dalrymple, S.A.; Dunn, J.; Freire-Moar, J.; Harris, S.; Labadie, S.S.; et al. Discovery of S-[5-Amino-1-(4-fluorophenyl)-1H-pyrazol-4-yl]-[3-(2,3-dihydroxypropoxy)phenyl]-methanone (RO3201195), an Orally Bioavailable and Highly Selective Inhibitor of p38 Map Kinase. *J. Med. Chem.* **2006**, *49*, 1562–1575. [CrossRef]
20. Bagley, M.C.; Davis, T.; Dix, M.C.; Murziani, P.G.S.; Rokicki, M.J.; Kipling, D. Microwave-assisted synthesis of 5-aminopyrazol-4-yl ketones and the p38MAPK inhibitor RO3201195 for study in Werner syndrome cells. *Bioorg. Med. Chem. Lett.* **2008**, *18*, 3745–3748. [CrossRef]
21. Röhm, S.; Berger, B.T.; Schröder, M.; Chaikuad, A.; Winkel, R.; Hekking, K.F.W.; Benningshof, J.J.C.; Müller, G.; Tesch, R.; Kudolo, M.; et al. Fast Iterative Synthetic Approach toward Identification of Novel Highly Selective p38 MAP Kinase Inhibitors. *J. Med. Chem.* **2019**, *62*, 10757–10782. [CrossRef] [PubMed]
22. Röhm, S.; Schröder, M.; Dwyer, J.E.; Widdowson, C.S.; Chaikuad, A.; Berger, B.T.; Joerger, A.C.; Krämer, A.; Harbig, J.; Dauch, D.; et al. Selective targeting of the αC and DGF-out pocket in p38 MAPK. *Eur. J. Med. Chem.* **2020**, *208*, 112721–112755. [CrossRef] [PubMed]
23. Fadaly, W.A.A.; Elshaier, Y.A.M.M.; Hassanein, E.H.M.; Abdellatif, K.R.A. New 1,2,4-triazole/pyrazole hybrids linked to oxime moiety as nitric oxide donor celecoxib analogs: Synthesis, cyclooxygenase inhibition antiinflammatory, ulcerogenicity, anti-proliferative activities, apoptosis, molecular modeling and nitric oxide release studies. *Bioorg. Chem.* **2020**, *98*, 103752–103771. [CrossRef] [PubMed]
24. Ibrahim, H.S.; Abou-Seri, S.H.; Tanc, M.; Elaasser, M.M.; Abdel-Aziz, H.A.; Supuran, C.T. Isatin-pyrazole benzenesulfonamide hybrids potently inhibit tumor-associated carbonic anhydrase isoforms IX and XII. *Eur. J. Med. Chem.* **2015**, *103*, 583–593. [CrossRef] [PubMed]
25. Pippione, A.C.; Sainas, S.; Federico, A.; Lupino, E.; Piccinini, M.; Kubbutat, M.; Contreras, J.M.; Morice, C.; Barge, A.; Ducime, A.; et al. N-Acetyl-3-aminopyrazoles block the noncanonical NF-κB cascade by selectively inhibiting NIK. *Med. Chem. Commun.* **2018**, *9*, 963–968. [CrossRef] [PubMed]
26. Hassan, A.Y.; Saleh, N.M.; Kadh, M.S.; Abou-Amra, E.S. New fused pyrazolopyrimidine derivatives; heterocyclic styling, synthesis, molecular docking and anticancer evaluation. *J. Heterocycl. Chem.* **2020**, *57*, 2704–2721. [CrossRef]
27. De, S.K. Pirtobrutinib: First Non-covalent Tyrosine Kinase Inhibitor for Treating Relapsed or Refractory Mantle Cell Lymphoma in Adults. *Curr. Med. Chem.* 2023; *ahead of print*. [CrossRef]
28. Schultze, M.D.; Reeves, D.J. Pirtobrutinib: A New and Distinctive Treatment Option for B-Cell Malignancies. *Ann. Pharmacother.* **2024**, 10600280231223737. [CrossRef] [PubMed]
29. Roskoski, R. Properties of FDA-approved small molecule protein kinase inhibitors: A 2024 update. *Pharmacol. Res.* **2024**, *200*, 107059. [CrossRef]

30. Mato, A.R.; Shah, N.N.; Jurczak, W.; Cheah, C.Y.; Pagel, J.M.; Woyach, J.A.; Fakhri, B.; Eyre, T.A.; Lamanna, N.; Patel, M.R. Pirtobrutinib in relapsed or refractory B-cell malignancies (BRUIN): A phase 1/2 study. *Lancet* **2021**, *397*, 892–901. [CrossRef]
31. Brandhuber, B.J.; Ku, N.C.Y.; Nanda, N.; Smith, S.A.; Tsai, D. Dosing of a Bruton's Tyrosine Kinase inhibitor. PCT Int. Appl. WO 2021113497, 10 June 2021.
32. Telaraja, D.; Kasamon, Y.L.; Collazo, J.S.; Leong, R.; Wang, K.; Li, P.; Dahmane, E.; Yang, Y.; Earp, J.; Grimstein, M.; et al. FDA Approval Summary: Pirtobrutinib for Relapsed or Refractory Mantle Cell Lymphoma. *Clin. Cancer Res.* **2024**, *30*, 17–22. [CrossRef]
33. Gomez, E.B.; Ebata, K.; Randeria, H.S.; Rosendahl, M.S.; Cedervall, E.P.; Morales, T.H.; Hanson, L.M.; Brown, N.E.; Gong, X.; Stephens, J.R.; et al. Pirtobrutinib preclinical characterization: A highly selective, non-covalent (reversible) BTK inhibitor. *Blood* **2023**, *142*, 62–72. [CrossRef]
34. Spallarossa, A.; Rapetti, F.; Signorello, M.G.; Rosano, C.; Iervasi, E.; Ponassi, M.; Brullo, C. Insights on pharmacological activity of imidazo-pyrazole scaffold. *ChemMedChem* **2023**, *18*, e202300252. [CrossRef]
35. Brullo, C.; Russo, E.; Garibaldi, S.; Altieri, P.; Ameri, P.; Ravera, S.; Signorello, M.G. Inside the Mechanism of Action of Three Pyrazole Derivatives in Human Platelets and Endothelial Cells. *Antioxidants* **2023**, *12*, 216. [CrossRef]
36. Benoit, G. Hydroxyalkyl hydrazines. *Bull. Soc. Chim. Fr.* **1939**, *6*, 708–715.
37. Schenone, S.; Bruno, O.; Ranise, A.; Bondavalli, F.; Brullo, C.; Fossa, P.; Mosti, L.; Menozzi, G.; Carraro, F.; Naldini, A.; et al. New pyrazolo [3,4-d]pyrimidines endowed with A431 antiproliferative activity and inhibitory properties of Src phosphorylation. *Bioorg. Med. Chem. Lett.* **2004**, *14*, 2511–2517. [CrossRef]
38. Lusardi, M.; Wehrle-Haller, B.; Sidibe, A.; Ponassi, M.; Iervasi, E.; Rosano, C.; Brullo, C.; Spallarossa, A. Novel 5-aminopyrazoles endowed with anti-angiogenetic properties: Design, synthesis and biological evaluation. *Eur. J. Med. Chem.* **2023**, *260*, 115727. [CrossRef]
39. Meta, E.; Brullo, C.; Sidibè, A.; Imhof, B.A.; Bruno, O. Design, synthesis, and biological evaluation of new pyrazolyl-ureas and imidazopyrazolecarboxamides able to interfere with MAPK and PI3K upstream signalling involved in the angiogenesis. *Eur. J. Med. Chem.* **2017**, *133*, 24–35. [CrossRef]
40. Zuo, S.J.; Li, S.; Yu, R.H.; Zheng, G.X.; Cao, Y.X.; Zhang, S.Q. Discovery of novel 3-benzylquinazolin-4(3H)-ones as potent vasodilative agents. *Bioorg. Med. Chem. Lett.* **2014**, *24*, 5597–5601. [CrossRef]
41. Lampe, T.; Alonso-alija, C.; Stelte-ludwig, B.; Sandner, P.; Bauser, M.; Beck, H.; Lustig, K.; Rosentreter, U.; Stahl, E.; Takagi, H. Substituted 4-benzyloxy-phenylmethylamide Derivatives as Cold Menthol Receptor-1 (cmr-i) Antagonists for the Treatment of Urological Disorder. PCT Int. Appl. Bayer Heatlthcare, WO 2006040136, 20 April 2006.
42. Singleton, V.L.; Orthofer, R.; Lamuela-Raventós, R.M. Analysis of total phenols and other oxidation substrates and antioxidants by means of Folin-Ciocalteu reagent. In *Methods in Enzymology*; Academic Press Ltd.: Cambridge, MA, USA; Elsevier Science Ltd.: London, UK, 1999; Volume 299, pp. 152–178.
43. Russo, E.; Spallarossa, A.; Comite, A.; Pagliero, M.; Guida, P.; Belotti, V.; Caviglia, D.; Schito, A.M. Valorization and Potential Antimicrobial Use of Olive Mill Wastewater (OMW) from Italian Olive Oil Production. *Antioxidants* **2022**, *11*, 903. [CrossRef]
44. Croce, K.; Libby, P. Intertwining of thrombosis and inflammation in atherosclerosis. *Curr. Opin. Hematol.* **2007**, *14*, 55–61. [CrossRef]
45. Cuesta, Á.M.; Palao, N.; Bragado, P.; Gutierrez-Uzquiza, A.; Herrera, B.; Sánchez, A.; Porras, A. New and Old Key Players in Liver Cancer. *Int. J. Mol. Sci.* **2023**, *24*, 17152. [CrossRef]
46. Taniyama, Y.; Griendling, K.K. Reactive oxygen species in the vasculature: Molecular and cellular mechanisms. *Hypertension* **2023**, *42*, 1075–1081. [CrossRef]
47. Alexander, Y.; Osto, E.; Schmidt-Trucksäss, A.; Shechter, M.; Trifunovic, D.; Duncker, D.J.; Aboyans, V.; Bäck, M.; Badimon, L.; Cosentino, F.; et al. Endothelial function in cardiovascular medicine: A consensus paper of the European Society of Cardiology Working Groups on Atherosclerosis and Vascular Biology, Aorta and Peripheral Vascular Diseases, Coronary Pathophysiology and Microcirculation, and Thrombosis. *Cardiovasc. Res.* **2021**, *117*, 29–42. [CrossRef]
48. Available online: http://dtp.cancer.gov (accessed on 30 March 2024).
49. Daina, A.; Michielin, O.; Zoete, V. SwissADME: A free web tool to evaluate pharmacokinetics, drug-likeness and medicinal chemistry friendliness of small molecules. *Sci. Rep.* **2017**, *7*, 42717–42729. [CrossRef]
50. Delaney, J.S. ESOL: Estimating Aqueous Solubility Directly from Molecular Structure. *J. Chem. Inf. Model.* **2004**, *44*, 1000–1005. [CrossRef]
51. Brenk, R.; Schipani, A.; James, D.; Krasowski, A.; Gilbert, I.H.; Frearson, J.; Wyatt, P.G. Lessons learnt from assembling screening libraries for drug discovery for neglected diseases. *ChemMedChem* **2008**, *3*, 435–444. [CrossRef]
52. Available online: https://comptox.charite.de/protox3/index.php?site=models (accessed on 30 April 2024).
53. Drwal, M.N.; Banerjee, P.; Dunkel, M.; Wettig, M.R.; Preissner, R. ProTox: A web server for the in silico prediction of rodent oral toxicity. *Nucleic Acids Res.* **2014**, *42*, W53–W58. [CrossRef]
54. Banerjee, P.; Dehnbostel, F.O.; Preissner, R. Prediction Is a Balancing Act: Importance of Sampling Methods to Balance Sensitivity and Specificity of Predictive Models Based on Imbalanced Chemical Data Sets. *Front. Chem.* **2018**, *6*, 362. [CrossRef]
55. Banerjee, P.; Eckert, A.O.; Schrey, A.K.; Preissner, R. ProTox-II: A webserver for the prediction of toxicity of chemicals. *Nucleic Acids Res.* **2018**, *46*, W257–W263. [CrossRef]
56. Mielnik, M.B.; Olsen, E.; Vogt, G.; Adeline, D.; Skrede, G. Grape seed extract as antioxidant in cooked, cold stored turkey meat. *LWT-Food Sci. Technol.* **2006**, *39*, 191–198. [CrossRef]

57. Aree, T.; Jongrungruangchok, S. Structure–antioxidant activity relationship of β-cyclodextrin inclusion complexes with olive tyrosol, hydroxytyrosol and oleuropein: Deep insights from X-ray analysis, DFT calculation and DPPH assay. *Carbohydr. Polym.* **2018**, *199*, 661–669. [CrossRef] [PubMed]
58. Maresca, M.; Colao, C.; Leoncini, G. Generation of hydrogen peroxide in resting and activated platelets. *Cell Biochem. Funct.* **1992**, *10*, 79–85. [CrossRef] [PubMed]
59. Born, G.V.R. Aggregation of blood platelets by adenosine diphosphate and its reversal. *Nature* **1962**, *194*, 927–929. [CrossRef] [PubMed]